PAPER NO: 123

Designing, manufacturing, and testing of sub- and supercritical composite shafts for helicopter tail drive line applications

by

H.Z. ter Wijlen (Urenco Nederland BV)

E. de Boer (University of Twente)

Urenco Nederland B.V.
P.O. Box 158, 7600 AD Almelo
The Netherlands

tel: +31 546 - 545911
fax: +31 546 - 818296

TWENTIETH EUROPEAN ROTORCRAFT FORUM
OCTOBER 4 - 7, 1994 AMSTERDAM

Printed by the Technical Highschool Haarlem

Designing, manufacturing and testing of sub- and supercritical composite shafts for helicopter tail drive line applications

H.Z. ter Wijlen (Urenco Nederland BV) and E. de Boer (University of Twente)

Urenco Nederland b.v.
P.O. Box 158, 7600 AD Almelo
The Netherlands

tel: +31 546 - 545911
fax: +31 546 - 818296

Abstract

Urenco Nederland has performed a feasibility study to design, manufacture, and test filament wound composite drive shafts for helicopter drive line applications. The drive shaft is a part of the drive line system of the helicopter, which transfers power from the main gear box to the tail rotor gear box. The shafts have to meet several requirements such as bending frequency, resist applied maximum torque, transfer of fatigue load during required life.

Formulas are presented which are very useful for a rough drive shaft design. The results of the optimization programme OPSHAFT and of an optimization with finite element models are given here. Most of the restrictions, assumptions and simplifications which are required to obtain analytical expressions are not needed for the FE model, which is a significant advantage.

Coupons, components, and full size sub- and supercritical shafts were manufactured, inspected and tested. The composite tubes are manufactured using the wet filament winding technique. An ultrasonic C-scan was used to gain insight into the laminate quality and extent of damage caused by impact and fatigue tests.

Coupon tests were performed to evaluate the laminate properties and joints. The component tests prove the residual strength after an impact or fatigue load. The full size shaft tests show the feasibility of the design with respect to dynamical behaviour, buckling, etc.

A composite drive shaft made by Urenco Nederland with the wet filament winding process is feasible and is characterized by:
- a highly automated process resulting in low recurring costs, a short production cycle, high reproducibility and reliability;
- a lower mass of the drive line system compared to one with metal shafts thanks to the composite material and the innovative design of the tools.
- low unbalance and perfect straightness

Contents

List of symbols

A	m^2	Cross sectional area
b_i	-	Coefficient i
CFRP	-	Carbon Fibre Reinforced Plastics
CLT	-	Classic Laminate Theory
CTD	^0C	Cold Temperature Dry
E	Nm^{-2}	Young's modulus
ETW	^0C	Elevated temperature wet
FPF	-	First ply failure
G	Nm^{-2}	Shear modulus
HM	-	High Modulus
I_x	m^4	Area moment of inertia
IGB	-	Intermediate Gear Box
ILS	Nm^{-2}	Inter Laminar Shear
IM	-	Intermediate Modulus
k	-	Shear correction factor (k=2 for thin-walled tube)
k_{bc}	-	Factor which includes imperfection, boundary conditions etc.
L	m	Length
m	kg	Mass
m'	kgm^{-1}	Mass per unit length
MGB	-	Main Gear Box
R	m	Mean radius of the tube
RTD	^0C	Room temperature dry
t	m	Wall thickness of the tube
TGB	-	Tail Gear Box
u,v,w	m	Displacement in direction x,θ,z
α		$\frac{\text{nominal speed}}{\text{1st critical speed}}$
λ_n	Hz	nth lateral eigenfrequency
ρ	kgm^{-3}	Density
ω_n	Hz	Nominal rotational speed

1 INTRODUCTION

Urenco Nederland has performed a feasibility study to design, manufacture, and test filament wound composite drive shafts for helicopter drive line applications. The drive shaft is that part of a helicopter's drive line system which transfers power from the main gear box to the tail rotor gear box.

Although the product resembles a simple thin-walled shaft, the design is a complex process, as it has to meet several conflicting requirements. Bending frequencies should be within the authorized frequency range. The shaft shall resist the applied torque without failure or torsional buckling. Even when damaged by impact, the shaft should be capable of transferring the fatigue load during the required life-time without failure. All this should be accomplished with a minimum mass and low life cycle cost.

In general, drive shaft designs are determined by instabilities (lateral eigenfrequency or torsional buckling) and so shafts made of materials with a high specific modulus (like composite) lead to a lower mass compared with metal shafts.

This paper describes the results of the feasibility study. The requirements are listed and the design approach is described including a case study for a drive shaft with an ultimate moment of about 1000 Nm. There is also a description of the manufacture and testing of sub- and supercritical shafts for an application with an ultimate moment of about 2000 Nm.

2 APPLICATION

The drive line transmits power from the main gear box (MGB) through the intermediate gear box (IGB) to the tail gear box (TGB). An outline of a drive line system is shown in figure 2.1. The components of the system are:

- main gear box
- tail gear box
- couplings
- drive shafts

Depending on the type, the following components are included:

- intermediate gear box
- intermediate bearing
- damper (not necessary for subcritical shafts)
- tail folding mechanism

The drive shaft consists of:

- flanges
- tube
- wear sleeve (optional for supercritical shafts)
- connecting parts (floating nuts, rivets, adhesive, etc. depending on the design solution).

The drive line system can be divided into sub-systems, for example MGB-IGB or IGB-TGB. Each sub-system can then be divided into one or more sections. The number of intermediate bearings and couplings required depends on the number of sections. It is clear, that the longer the shaft, the higher the mass gain of the total system.

3 REQUIREMENTS

Requirements for geometry envelope, vibrations, damage tolerance, (environmental) loads, and masses shall be accomplished with a cost effective drive shaft.

Geometry envelope

The size of the shaft should not exceed the described envelope outline. Generally the diameter of the couplings defines the limit of the outer diameter of the shafts.

Vibrations

The drive shafts are a part of the total system in which torsional, axial, and lateral frequencies occur. The torsional system can be reduced to a simplified one in which the shaft's torsional stiffness is important. The requirement for this is the torsional stiffness of the tube. Axial frequencies are usually not considered while lateral frequencies are the design drivers. The lateral frequencies allowed are specified with a so called authorized frequency range. To avoid shaft whirling, the nominal speed shall operate at a certain distance from the lateral eigenfrequencies of the shafts. The authorized frequency range is also influenced by additional requirements to avoid interference with other eigenfrequencies of the helicopter (see the example in figure 3.1).

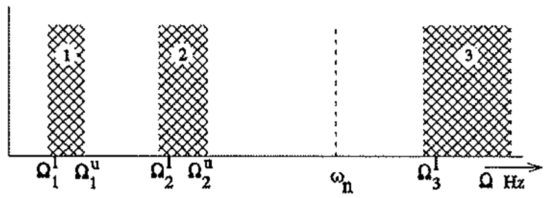

Figure 3.1 Outline of the authorized ranges for lateral frequencies

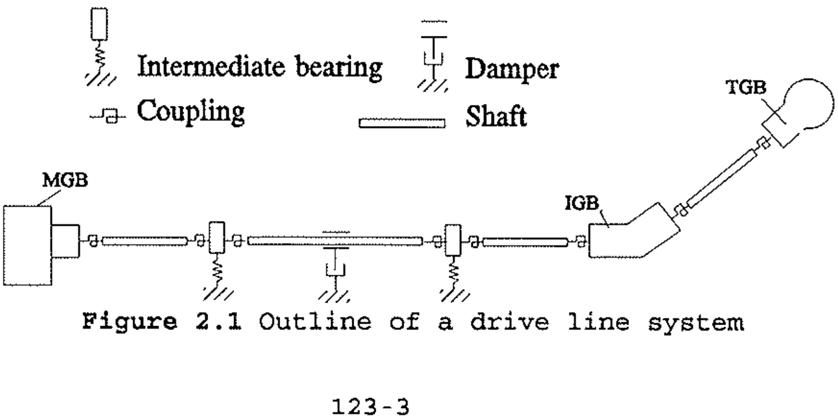

Figure 2.1 Outline of a drive line system

Damage tolerance

The damage tolerance (fail-safe) requirement of a structure requires that if damage (fatigue, intrinsic/discrete damage, large area manufacturing flaws, or severe) should occur during the operational life of the helicopter, the remaining structure shall withstand reasonable loads without failure or excessive structural deformation until the damage is detected, see *FAA - AC 20 - 107 A*.

Low velocity impact damage is caused by tool drop and is simulated by impacting with a prescribed energy level. High velocity impact tolerance is required for military applications. A so called "get home load" is defined after ballistic impact.

Environmental conditions

The shafts shall withstand, without malfunction, deterioration or breakdown, the following environmental conditions:

- sand and particles as encountered in a desert
- exposure to salt sea atmosphere
- relative humidity to 100 %
- temperature range from a certain minimum to a certain maximum level
- a certain altitude range.

Furthermore the shaft shall be able to transfer a certain load at an increased temperature level during a limited time; this is also called the heat resistance requirement.

In general the following loads are possible:

- axial forces
- radial forces
- bending moments
- torsional moments
- body loads due to rotation or acceleration

The misalignment causes radial loads and bending moments in the drive line system. Due to the application of couplings, these loads give low stresses compared to torsional moments. Thus the dominating load for the drive shaft is the torsional moment. The limit load is derived from the maximum load level of a certain service spectrum. The ultimate load level is a safety factor times limit load level. A certain service spectrum leads to a fatigue load in the drive line system.

Mass and cost target

The drive line system with composite shafts shall be competitive with the drive line system consisting of metal shafts with respect to mass and cost. The comparison may not be restricted to the shafts only, but has to include the total drive line system. For example, a shaft with an increased length may reduce the required number of couplings, flanges, intermediate bearings with support and monitoring systems.

4 DESIGN

4.1 DESIGN APPROACH

Fibre

Combinations of various types of fibres are possible, for example a combination of glass fibre with a High Modulus (HM) carbon fibre. The carbon fibres will create a sufficiently high stiffness level, the damage tolerance requires a high strain fibre. Another advantage of composites is the superior fatigue performance compared to metals. The amount of fibre types gives an additional degee of freedom to optimize the design with respect to stiffness, strength, stability, fatigue and damage tolerance. The carbon fibre used was an Intermediate Modulus (IM) type, which was a compromise for both properties.

Resin

The resin should have good resistance in chemical, thermal and humid conditions and have a sufficiently high strain fracture level in combination with the fibre applied. A high curing epoxy can be applied in the wet filament winding technique.

Tube dimensions

The goal is to have a cost effective drive line system with a low number of different parts, a design which has damage tolerance, and a low mass. The design for the various shaft types may have:

- the same internal tube diameter throughout the system
- the same lay-up pattern
- the same flanges

The advantages are:

- fewer qualification activities
- higher margin of safety for some parts
- larger production lot (results in reduced manufacturing cost)
- lower manufacturing tool cost (same mandrel diameter, etc.)

The disadvantage is a slight increase in mass.

The basic design approach is to optimize the drive line with:

- firstly: different diameters and lay-up patterns
- secondly: equal diameter and different lay-up patterns
- thirdly: equal diameter and equal lay-up patterns

The final choice is based on the amount of increase in mass, considering the total life cycle cost.

Metal flange - composite tube connection

The shaft consists of a cylindrical composite tube, which is connected to a metal flange. The flange and the tube can be joined by:

- adhesive bonding
- mechanical fasteners (rivets or bolts)
- shrinkage
- a polygon connection, see *Nohr*
- a combination of above options

The choice of connection is based on high reliability, damage tolerance, qualification process (cost), etc. Mechanical fasteners were chosen for the feasibility study.

Damage tolerance

The so called "no damage growth concept" is used for the damage tolerance evaluation. The objective of this approach is to set the design strains in such a way that should intrinsic and discrete source damage occur within the operational life of the structure, these defects/damages will not propagate under the anticipated service spectrum.

4.2 BASIC EQUATIONS

Three constraints are assumed to be critical for shaft design: lateral frequency, torsional buckling, and torsional material strength.

Lateral frequency

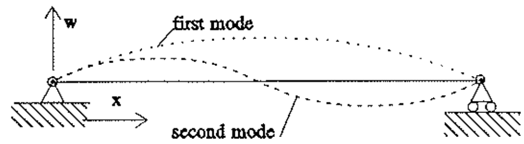

Figure 4.1 Shaft modelled as a hinged supported beam.

As a first estimate for the lateral frequency calculation the shaft was modelled as a hinged beam (see figure 4.1). The lateral eigenfrequencies can be obtained according to the Timoshenko beam theory which accounts for the effect of shear deformation and rotary inertia, see *Timoshenko*. These effects are omitted for the Euler-Bernoulli beam theory. The beam deformation can be described with the following equation:

$$E_x I_{xw}^{////} + \rho I_x \lambda_n^2 \left(1+\frac{kE_x}{G}\right) w'' - \rho A \lambda_n^2 w = 0$$

$$\text{with} \quad w' = \frac{\partial w}{\partial x} \qquad (4\text{-}1)$$

boundary conditions:
$w(x,t) = w'' = 0$ at $x = 0, L$

The general solution for the n^{th} bending frequency is:

$$\lambda_n = \frac{b_n}{\pi}\frac{R}{L^2}\sqrt{\frac{E_x}{8\rho}} \quad [Hz] \qquad n = 1, 2, ..$$

(4-2)

The coefficients b_n for the Timoshenko theory are equal to:

$$b_n = \frac{n^2\pi^2}{\left[1+\frac{n^2\pi^2}{2}\left(\frac{R}{L}\right)^2\left(1+\frac{kE_x}{G}\right)\right]^{1/2}} \qquad (4\text{-}3)$$

Torsional buckling

Drive shafts with a large (L/R) ratio and thin walls are susceptible to torsional buckling. Different buckling theories are available from the literature, for tubes of "moderate" or "long" length and for isotropic or orthotropic materials, see *Simitses* and *Timoshenko*. The influence of the boundary conditions is only noticeable in moderately long tubes, not in long tubes. The dimensionless Batdorf parameter is encountered to validate the applicability of buckling formulas:

$$Z = \left(\frac{E_x}{E_\theta}(1-\nu_{x\theta}\nu_{\theta x})\right)^{1/2} \frac{L^2}{Rt} = (1-\nu^2)^{1/2}\left(\frac{L}{R}\right)^2 \frac{R}{t} \qquad (4\text{-}4)$$

The Simitses solution for torsional buckling is used in most references for drive shafts (see *Abrate*, *Hermens*, *Lim*, etc.) It may be applied for tubes of moderate length and is equal to:

$$M_{cr} = \frac{\pi^3}{6}\, k_{bc} \cdot \frac{R^{5/4} t^{9/4} E_x^{3/8} E_\theta^{5/8}}{(1-\nu_{x\theta}\nu_{\theta x})^{5/8} L^{1/2}} \qquad (4\text{-}5)$$

$$\text{conditions:} \quad 10^2 \le Z \le 10^5$$

The value k_{bc} includes the influence of imperfections, difference theory with experimental and boundary conditions, see *Fuchs*. A value of 0.7 is used in this paper. The buckling modes are shown in figure 4.2.

The Timoshenko buckling solution is applied for long shafts with quasi-isotropic material behaviour:

$$M_{cr} = 0.165 \frac{2\pi E}{(1-\nu^2)^{3/4}} \cdot R^{1/2} t^{5/2} \qquad (4\text{-}6)$$

$$\text{condition:} \quad Z \ge 44\left(\frac{R}{t}\right)^2 (1-\nu^2)$$

A value of 0.7 is also used in this equation.

Torsional material strength

In general, a shaft is subjected to several loads and must be evaluated to avoid material failure. To do this, the loads are transformed to the ply stresses via the classical laminate theory (CLT) and these stresses are evaluated against a suitable failure criterion, see *Tsai*. In this paper only the torsional material strength is assumed to be critical and the stresses and strains can be evaluated against the allowable stresses and strains with the maximum stress, maximum strain, Tsai-Wu criteria, etc.

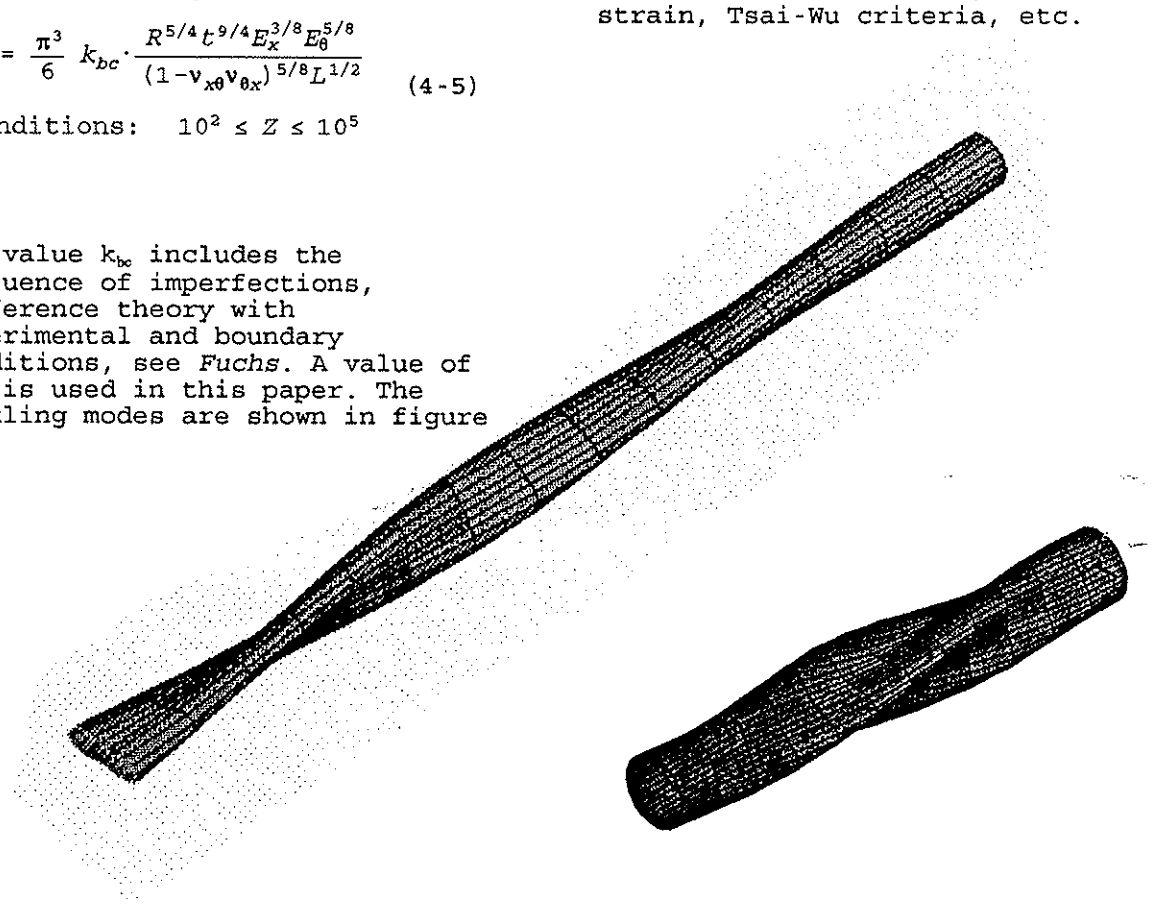

Figure 4.2 Long shaft and shaft of "moderate length" buckling modes

4.3 SIMPLIFIED ANALYTICAL ESTIMATE

An analytical solution is derived for the mass per unit of length if the lateral frequency and torsional buckling requirements are critical. It is assumed that the strength is not critical. Once the mass is known, the values for the design variables radius and wall thickness can be obtained by substituting the mass into the appropriate equations. The mass per unit of shaft length is:

$$m' = 2\pi\rho R t \qquad (kg/m) \qquad (4\text{-}7)$$

The two design variables, radius and wall thickness, are eliminated by substitution of the formula for the lateral frequency and torsional buckling, respectively. Furthermore, the following relationship between the frequencies is used, based on the Euler-Bernoulli theory:

$$\lambda_n = \frac{b_n}{b_1}\lambda_1 = n^2 \lambda_1 \qquad (4\text{-}8)$$

The lowest weight is obtained when the first critical speed is as low as possible compared to the nominal speed. A safety margin of 20 % is used between the nominal speed and the critical speed above the nominal speed. The following formula is used:

$$\omega_n = (0.8)\,\lambda_n = \alpha\,\lambda_1 \qquad \text{with } \alpha = (0.8\, n^2) \qquad (4\text{-}9)$$

Two mass estimation formulas were obtained for both buckling formulas:

1 Timoshenko - long tube

$$m' = 5.69\left\{\frac{M^2\,\omega_n^4 L^8\,(1-\nu^2)^{3/2}\rho^7}{\alpha^4\,E^4}\right\}^{1/5} \qquad (4\text{-}10)$$

$$\text{condition:}\quad Z \geq 44\left(\frac{R}{t}\right)^2 (1-\nu^2)$$

2 Simitses - moderate length

$$m' = 3.39\left\{\frac{M^4\,\omega_n^4\,(1-\nu_{x\theta}\nu_{\theta x})^{5/2} L^{10}\rho^{11}}{\alpha^4\,E_x^{7/2}\,E_\theta^{5/2}}\right\}^{1/9}$$

$$\text{condition:}\quad 10^2 \leq Z \leq 10^5 \qquad (4\text{-}11)$$

To demonstrate the use of the formulas, the following simplifications were made for the composite shaft material compared with aluminium shafts: the

Number of critical speeds below nominal speed	Aluminium drive shafts			CFRP drive shafts		
	dia-meter	strength	mass	dia-meter	strength	mass
0	1	1	1	0.77	1.5	0.53
1	0.25	7.4	0.54	0.19	11	0.28
2	0.11	24	0.38	0.09	35	0.20

Table 4.1 Dimensionless data for drive shafts of intermediate length

Number of critical speeds below nominal speed	Aluminium drive shafts			CFRP drive shafts		
	dia-meter	strength	mass	dia-meter	strength	mass
0	1	1	1	0.77	1.6	0.48
1	0.25	12	0.33	0.19	19	0.16
2	0.11	52	0.17	0.09	84	0.08

Table 4.2 Dimensionless data for long drive shafts

stiffness is of similar level and the density ratio equals 0.60 (≈1600/2700). The diameter, torsional strength and mass per unit of length are made dimensionless with the values of aluminium sub-critical. The results of these formulas are given in table 4.1 for shafts of moderate length and in table 4.2 for long shafts. The tables show clearly that the use of composite shafts results in a mass reduction of about 50 % with a radius of 77 % and an increased stress level compared to aluminium.

The restriction of the derived formulas was that the strength is not critical in the application, however this assumption has be checked.

The derived formulas can also be used for other trade-off studies. In general, two or more aluminium shafts are replaced by a lower number of composite shafts. The formulas show that replacing three aluminium shafts with two composite shafts of increased length gives a similar mass per unit of length.

4.4 OPSHAFT

A computer programme, OPSHAFT, has been developed at Urenco Nederland to perform a fast and efficient optimization of a metal or multi-layered composite **shaft**.

The programme OPSHAFT:
- minimizes the objective function (the mass)
- complies with requirements for stiffness, strength, and lateral eigenfrequency where possible
- optimizes the design variables within their constraints.

The design variables are the radius, thicknesses, and winding angles of each ply. An extended Timoshenko beam theory was applied to calculate the lateral frequencies. The Simitses formula was used to calculate the critical buckling load with k_{bc}= 0.7. The ply stresses from the tube loads were evaluated using CLT and first ply failure (FPF).

OPSHAFT was used for a case study in which the shaft length was about 2000 mm and the torsional load approximately 2000 Nm. The comparison of a subcritical aluminium shaft and composite shaft is shown with dimensionless values in figure 4.3. These results compare well with the results of the simplified analytical estimate (see table 4.1). Moreover the figure shows that the tube diameter is an additional design option.

4.5 OPTIMIZATION WITH FE MODELS

A general design tool is the optimization based on finite element calculations of the objective function and state variables. The objective function

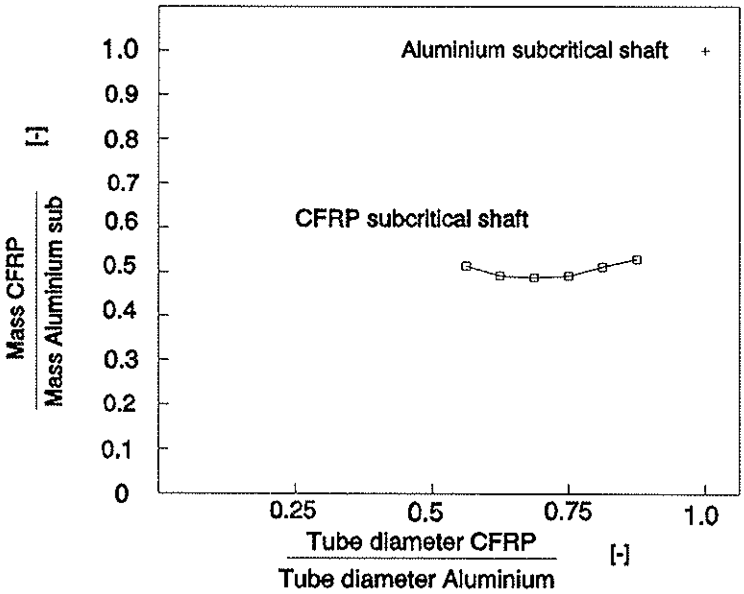

Figure 4.3
Dimensionless comparison of CFRP with aluminium shafts

and state variables can be the same as for the programme OPSHAFT. The result of the optimization is a new, optimal design that has been checked for feasibility. The major advantage is that most of the restrictions, assumptions and simplifications required to obtain analytical expressions are not necessary when optimizing FE models. The influence of the stacking sequence was considered with the FE model. It was not estimated with uniform material properties through the thickness. Analysis showed that the metal wear sleeves act as a local reinforcement and increase the linear torsional buckling moment by 10 %. These and other influences on mass and stiffness can easily be incorporated in the FE model. One drawback of this method is the time-consuming computation for each design.

The ANSYS FE models, one model per state variable, were built with a 8-node layered shell element. The FE model for the lateral frequency is a hinged thin-walled tube (see figure 4.1). For torsional buckling and torsional strength, the FE model is a thin-walled circular cylindrical shell with clamped end conditions. In chapter 5 you can see how the FE optimization is applied in the case study.

5 CASE STUDY

5.1 General

A drive line optimization was performed for a case study and some results are presented in this chapter. Several drive line types can be composed depending on the number of shafts per section and the subcritical or supercritical speed. For each of these shafts the design was estimated with the simplified analytical formulas and calculated with the programme OPSHAFT. Furthermore, an optimization with FE models was performed for one type of drive line. A brief evaluation was made of the design procedure.

5.2 REQUIREMENTS

The design requirements can be summarized as follows:
- authorized frequency spectrum, similar to figure 3.1
- nominal operation speed ω_n
- maximum ultimate moment M_{cr}=1000 Nm
- sub system length of ≈ 5000 mm

The critical speed of a shaft may be such that the first critical speed is in the first, second or third authorized frequency range.

Number of sections	Number of critical speeds below nominal speed	formula 4-10 (Simitses)		formula 4-11 (Timoshenko)	
		Aluminium	CFRP	Aluminium	CFRP
3	0	3.6	1.9	4.0	1.9
2	0	5.7	3.0	7.6	3.6
	1	3.1	1.6	2.5	1.2
	2	2.2	1.1	1.3	0.6
1	1	6.7	3.5	7.6	3.6
	2	4.6	2.5	4.0	1.9

Table 5.1 Estimation of the total mass of the shafts [kg]

5.3 SIMPLIFIED ANALYTICAL ESTIMATE

The mass of the shaft was estimated with the simplified analytical formulas. For the results see table 5.1.

5.4 OPSHAFT OPTIMIZATION

The results of an OPSHAFT optimization are given in table 5.2. Also the weight of other parts are included, so a trade-off based on mass can be made. The design with one section and composite shaft, which passes two critical speeds below nominal speed, gives the lowest mass. The composite shaft weighs 3.3 kg less than the three subcritical aluminium shafts. However, the weight saving in the other parts (bearings, couplings etc) is as much as 9.6 kg. Comparison of shaft mass with the simplified analytical estimations based on buckling and frequency of table 5.1 gives acceptable estimates of the masses.

5.5 FE OPTIMIZATION

For one type an optimization was carried out with FE models. Compared with the OPSHAFT optimization, the safety margin for torsional buckling is reduced to 10 % due to fewer assumptions and restrictions of the FE model. The long twofold supercritical composite shaft for one section with a mass of 2.4 kg according the OPSHAFT optimization (see table 5.2) is futher optimized to a mass of 1.65 kg (which is an additional mass saving of ≈ 30 %)! This additional reduction of mass is caused by:
- a lower safety margin of 10 % compared to 30 % in OPSHAFT for torsional buckling (mass reduction of ≈ 10 %)
- the use of an FE buckling model instead of the Simitses approach for torsional buckling
- the influence of stacking sequence.

The simplified analytical mass estimate based on the Timoshenko approximation shows less deviation (≈ 15%) compared to the FE optimization than the Simitses approximation (≈ 35%), see table 5.1.

Number of sections	Number of critical speeds below nominal speed	mass of Aluminium design (kg)		mass of CFRP design (kg)	
		shafts	total mass	shafts	total mass
3	0	5.7	17.4	2.0	13.7
2	0	6.3	12.5	3.0	9.2
	1	3.2	11.5	2.0	10.3
	2	NA	NA	NA	NA
1	1	7.0	8.4	3.3	4.7
	2	4.9	7.0	2.4	4.5

NA= not applicable, meaning that no design exists for the given constraints

Table 5.2 Mass of the shafts and sub system [kg] calculated with OPSHAFT

6 MANUFACTURING AND INSPECTION

For another case study the section between the MGB and the IGB could be done for example with three subcritical shafts or two super-critical shafts. To show the feasibility of the composite shafts for that application, coupons, components and full-size sub- and supercritical shafts have been manufactured and tested.

Tube

The tubes were manufactured using the wet filament winding technique. During this winding process one or more tows of fibre, which are impregnated with resin, are wound on a mandrel. After the winding process, the composite is cured on the mandrel and in the furnace following a qualified procedure with respect to temperatures and times. The result is a fibre reinforced plastic tube. The wet filament winding process has been further optimized at Urenco Nederland especially for low unbalance and perfect straightness of thin-walled tubes. The following tools and machines were used:
- a 4-axis machine with a maximum length of 5 m and maximum lay-up with 4 tows simultaneously
- an aluminium mandrel with inside heating
- a steel mandrel with external heating
- an oven for the gelling and curing process
- grinding machines to cut the tubes to length

Flange and tube-flange connection

The metal flanges have been turned. The tube-flange connection consists of mechanical fasteners. The tools and machines are:
- an assembly-jig to assemble flanges within tolerances on length and parallelism, to ensure the interchangeability of shafts
- a drilling machine with special drills to go through carbon and metal with small tolerances
- a riveter

A picture of the test component is shown in figure 6.1.

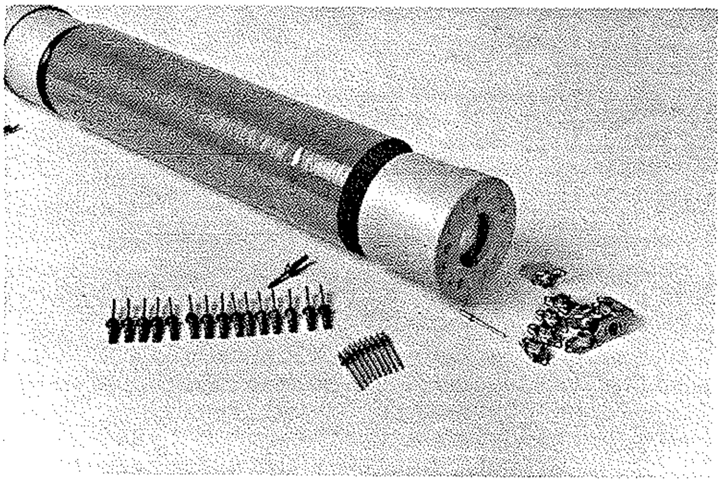

Figure 6.1 Test component

Inspection technique

During the development phase an ultrasonic C-scan was used (see figure 6.2) to gain insight into the laminate quality regarding such phenomena as voids, delaminations, blisters and inclusions. Furthermore this technique is used to determine the extent of damage to test articles used during low and high velocity impact damage and fatigue tests.

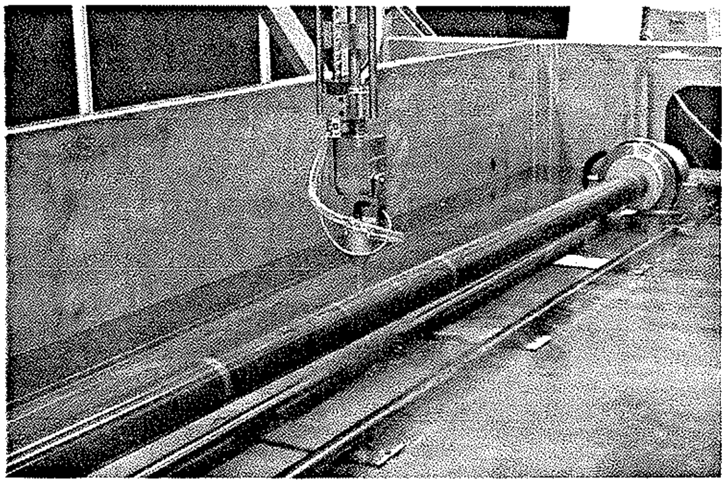

Figure 6.2 Shaft in C-scan

7 TESTING

7.1 GENERAL

A test programme has been carried out in which coupons, components and full size shafts were tested and evaluated. The coupon tests (small specimens) were performed to evaluate the laminate properties or mechanically fastened joints to obtain the knock down factors and generation of "A" or "B" design allowables. The "A" base design allowable is the value above which at least 99% of the population of values is expected with a confidence of 95%. The "B" base design allowable is the value above which at least 90% of the population of values is expected with a confidence of 95%. The component tests (short tubes with flanges) are performed for evaluation of the connection or tube residual strength after an impact or fatigue load. The full size shaft tests are performed to show the feasibility of the design with respect to dynamical behaviour, buckling after an impact damage, etc.

7.2 COUPON

The various environmental conditions are shown in table 7.1. Other tests were also carried out on coupons, fibres and resin but not under all the environmental conditions stated in table 7.1.

Coupon testing	Exposure		
	CTD	RTD	ETW
Compression	x	x	x
In plane shear	x	x	x
ILS	x	x	x
flexural	x	x	x
bearing	x	x	x

Table 7.1 Test matrix of coupon testing

7.3 COMPONENT

At component level (see figure 6.1) the following tests were performed:
- threshold of detectability determination on short tubes
- fatigue test on the connection with residual strength tests
- low velocity impact damage tests with residual strength tests
- high velocity impact damage tests with residual strength tests.

An additional layer was applied to the outside of some tubes. This layer, which consisted of a thin glass-epoxy layer was meant to reduce the threshold of the detectability level. The influence of surfaces was investigated with eight tubes, each tube having an impact of 20 Joule. Four of the eight tubes had an additional glass layer. These showed visible damage on the outside of the tube, see figure 7.1.

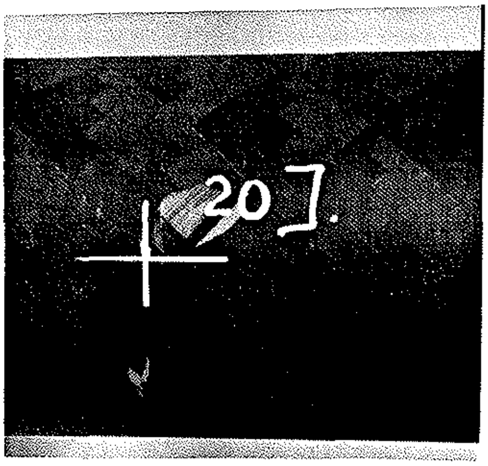

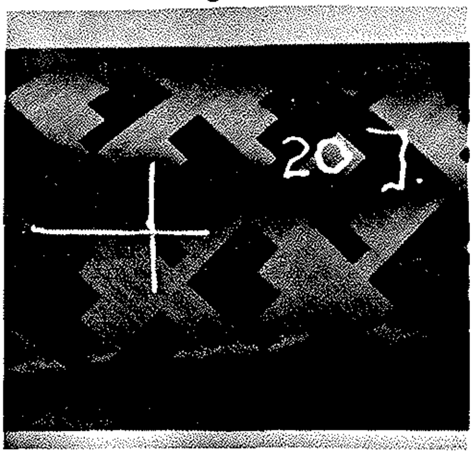

Figure 7.1 Two surfaces which are impacted with 20 Joule

Six tube flange connections were successfully loaded with a fatigue load of 960 Nm, min/max ratio of 0.1 and a million cycles. Residual strength tests were performed at two connections. One connection failed at a level of 4000 Nm and the other did not fail even at 5000 Nm (maximum level of the test equipment).

Low velocity impact tests were performed with three levels of impact: 10, 20 and 40 Joule. The results of the residual torsional strength test of three test components are presented in table 7.2.

Impact level [Joule]	Residual strength [Nm]
0	4350
10	2460
20	2026
40	1313

Table 7.2 Residual torsional strength test results

High velocity impact tests were performed with two types of bullets. Important is the position of the impact on the shaft. Three positions were tested: through the centre, tangential to the tube, and a position between these two. Residual strength tests were carried out with the test components. You can see the back of the components in figure 7.2; the subcritical shaft has a larger diameter compared to the supercritical shaft and the damaged area is local. The supercritical shaft has relatively much more damage.

7.4 FULL SIZE SHAFT

The ultimate torsional load requirement was about ≈ 2000 Nm. The global dimensions of the subcritical shaft are:
diameter: ≈ 140 mm
length: ≈ 2300 mm
mass: ≈ 1.1 kg/m

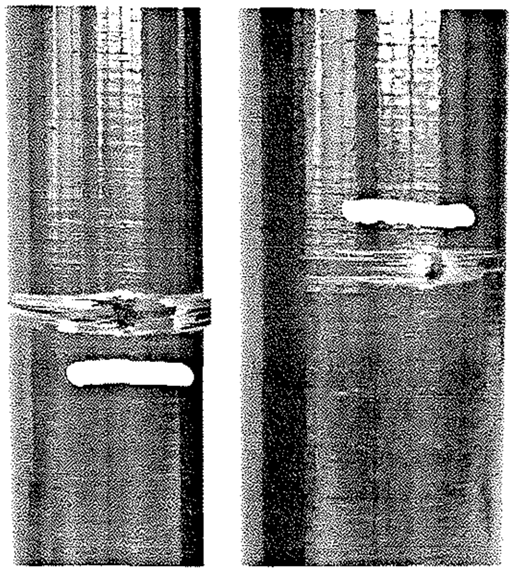

Figure 7.2 View of the back of the component with ballistic damage

The following tests were performed on a full size shaft:
-the influence of torsional moment on lateral eigenfrequency level
-the influence of holes on the torsional buckling moment level

The measured lateral eigen-frequencies of the shaft compared well with the theoretical predicted values, the deviation being less than 2 %. The lateral frequencies were also measured when the shaft was loaded with the limit load level, and the change in eigenfrequency was negligible.

Two diametral holes were drilled to simulate a ballistic impact. Buckling tests were performed with different sizes of holes. The results are summarized in table 7.3. The shaft showed a strength failure at a level of 3200 Nm.

Hole size diameter [mm]	Torsional buckling moment [Nm]
0	3400
10	3370
20	3340
30	>3200

Table 7.3 Torsional buckling moment

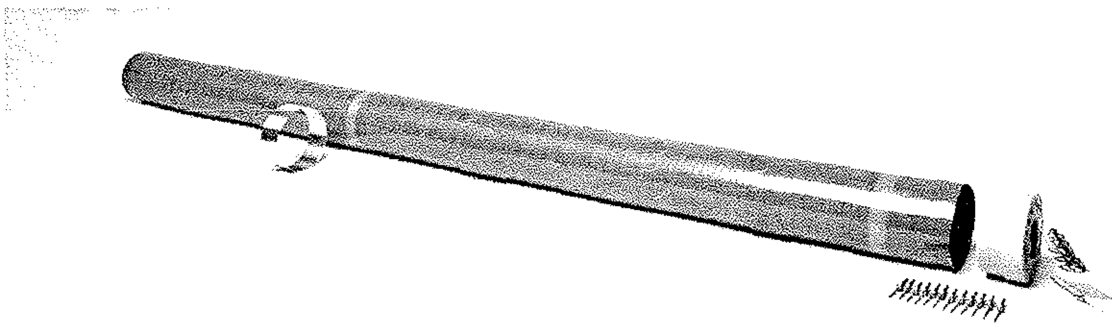

Figure 7.3 Supercritical shaft parts

The global dimensions of the supercritical shaft are:
diameter : ≈ 90 mm
length: ≈ 3200 mm
mass: ≈ 0.8 kg/m
The shaft is shown in figure 7.3.

The following test sequence was performed at one shaft:
- modal analysis (lateral eigenfrequency)
- dynamical behaviour (passing critical frequency)
- buckling moment
- low velocity impact damage of 25 Joule
- fatigue load simulating infinite life time
- residual strength

Between the test activities, a C scan investigation was performed to check the size and growth of the damage after fatigue loading.

The shaft passed the critical frequency without any problem with an eigenfrequency at the predicted level. The buckling moment was equal to 4050 Nm. The torsional testrig is shown in figure 7.4. A low velocity impact test was performed with 25 Joule. In order to simulate a certain life-time, the shaft was loaded with a fatigue spectrum. After fatigue loading, the size of the damaged area did not increase. The residual strength was above the ultimate load level.

The buckling moments of the sub- and supercritical shaft deviate less than 5 % compared to the predicted theoretical values.

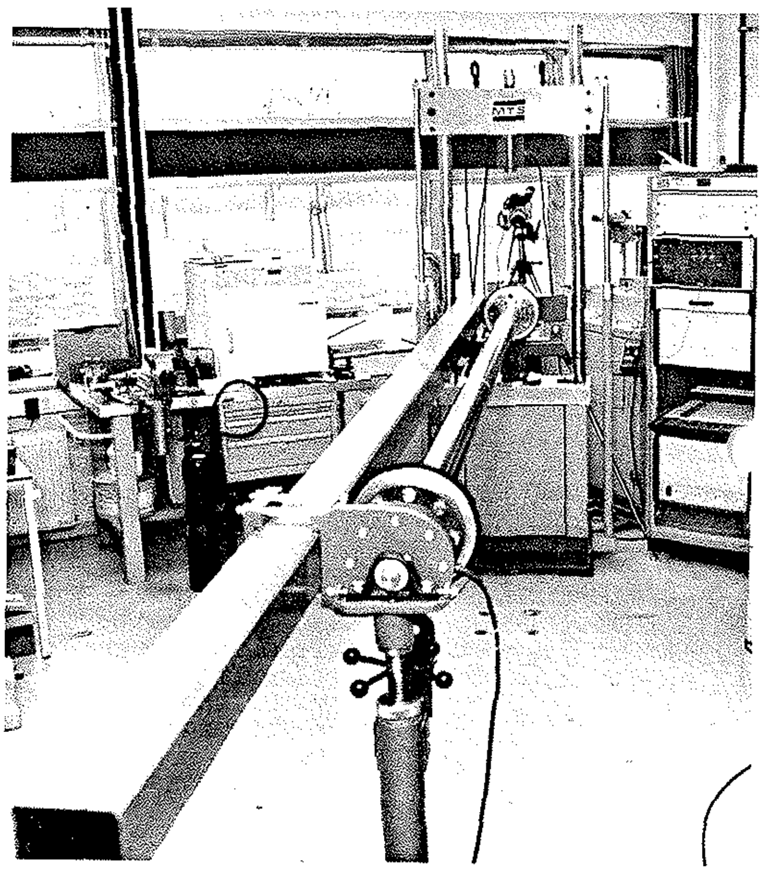

Figure 7.4 Torsional test rig

8 CONCLUSIONS

In this paper, formulas are presented which are very useful for making a rough estimate of a drive shaft design. The mass per unit of length for a shaft of moderate length can be estimated with formula 4-11. The mass per unit of a long shaft can be estimated with formula 4-10.

Composite shafts made of IM carbon fibre and epoxy resin give a reduction of about 50 % compared with aluminium shafts.

Composite shafts give the designer additional freedom in choosing the diameter within certain constraints.

The formula of Simitses for torsional buckling, which is frequently used in the literature, cannot be used for long shafts.

A composite drive shaft made by Urenco Nederland with the wet filament winding process is feasible and is characterized by:

- a highly automated process resulting in low recurring cost, short production time, high reproduceability and reliability;
- a lower mass of the drive line system compared to a drive line system with metal shaft as a result of the composite material and the innovative design equipment.
- low unbalance and perfect straightness

9 REFERENCES

S. Abrate
Composite Driveshaft Designs
SAE paper 891031, General aviation aircraft meeting and exposition

Federal Aviation Administration
Composite Aircraft Structure
Advisory Circular 20-107A

W.P. Fuchs, et al.
CFRP Precision-wound tubes in aerospace engineering
Paper 19, Sampe London 1983

E. Hermens and N. Verschuren
New transmission components for helicopter applications
Paper 19, Fifteenth European Rotorcraft Forum, 1989, Amsterdam

J.W. Lim and Darlow
Optimal sizing of composite power ransmission shafting
Journal of the American Helicopter Society, jan. 1986, pp 75 -83

M. Nohr
Thin-walled composite tubes with non-circular sections in torsion
36th International Sampe Symposium and exhibition, 1991, pp 733 - 743.

G.J. Simitses
Instability of Othortropic Cylindrical Shells under Combined Torsion and Hydrostatic Pressure
AIAA Journal, Vol.5, No.8, August 1967

G.J. Simitses, et al.
The accuracy of Donnel's equations for axially-loaded, imperfect orthotropic cylinders
Computers & Structures, Vol.20,No. 6, pp. 939 -945, 1985

P. Timoshenko, J. Gere,
Theory of Elastic Stability
Second edition, McGraw-Hill Book Company, 18th printing, 1986

S. Tsai
Composite Design
Think Composites, Ohio, USA, fourth edition, 1988